OPTOELECTRONİCS AND ADVANCED MATERİALS – RAPİD COMMUNİCATİONS Vol. 3, No. 4, April 2009, p. 383 - 389

Studies on properties of sprayed SnO_2 thin films as a function of substrate-nozzle distance and substrate temperature

E. GÜNERI, C. GÜMÜŞ[a*] , F. MANSUR[a], F. KIRMIZIGÜL
Department of Primary Education, University of Erciyes 33039 Kayseri, Turkey
[s]*Physics Department, University of Cukurova 01330 Adana, Turkey*

Transparent polycrystalline tin oxide (SnO_2) thin films were deposited on commercial microscope glass substrates using spray pyrolysis method. Thin films were deposited at various nozzle-to-substrate distances from 20 to 40 cm in steps of 5 cm and at various substrate temperatures ranging between 380 to 440 °C in steps of 20 °C. The thin films are found to have a tetragonal rutile structure. Lattice parameters were calculated as a = 4.74 Å and c = 3.18 Å. The surface morphology of the films were imaged by SEM (Scanning Electron Microscope). The average grain size of the films obtained were 22.3-74.8 nm by using Scherrer's formula. The films were found to exhibit high transmittance >90 % in the visible regions. Absorption coefficient α and the thickness of the film t were calculated from interference of transmittance spectra. Refractive index n and extinction coefficient k were determined from transmittance spectrum in the ultraviolet-visible-near infrared regions using envelope methods. The refractive index is found to vary between 1.76-1.92 in the wavelength range of 400-1100 nm. The values direct band gaps of the films obtained were 3.99-4.11 eV. The electrical resistivity (ρ) of the films obtained were (2.47-7.13)·10^{-4} Ωcm by using Ohm's law.

(Received April 09, 2009; accepted April 23, 2009)

Keywords: Tin oxide, Spray pyrolysis method, Thin films, Refractive index

1. Introduction

Metal oxide thin films have been studied in the last decade for application in various fields such as solar cells, opto-electronic devices, liquid crystal displays, heat mirrors and gas sensors. Undoped and doped non-stoichiometric metal oxide thin films have a high optical transparency in the visible spectrum and have a conductivity near to that of metals [1,2]. Among these oxide thin films, SnO_2 thin films have been known to be chemically and thermally stable in atmospheric environment and mechanically harder than ZnO thin films. SnO_2 has a higher resistivity than ITO and a higher optical transmission than CdO. Specifically, the thickness of the transparent conductive SnO_2 film should be 5000 Å or larger [3, 4]. Tin oxide thin films, which have a wide energy band gap, are transparent n-type semiconductors. The crystal structure of SnO_2 thin films was found by observing its X-ray diffraction pattern, It was determined as tetragonal [5]. There is comprehensive literature on tin oxide films prepared on glass substrates by different techniques, e.g. RF sputtering technique [6], sol-gel method [7], chemical bath deposition [8], pulsed laser deposition [9] and spray pyrolysis [10,11,12]. Spray pyrolysis method is one of the best known simple chemical techniques to prepare a variety of thin films such as noble metals, metal oxides and chalcogenide compounds. In this method, the thin film is formed by spraying a solution on a heated substrate where the constituents react to form a chemical compound. The chemical reactants are selected so that products except the desired compounds are volatile at the temperature of deposition. The chemical reactants should be appropriately selected, otherwise products expect the desired compound may form in thin films [11,12].

This paper deals with structural, optical, and electrical properties of SnO_2 thin films prepared by spray pyrolysis at different substrate-to-nozzle distances and different substrate temperatures. The crystallinity and structure of the films were investigated by X-ray crystallography. A scanning electron microscope was used to view the variations of the films topological properties. The optical properties were determined by a spectrophotometer. Using these results, it was found how thin films were affected by the substrate-to-nozzle distance and substrate temperature, during deposition.

2. Experimental procedure

The solution, consisting of $SnCl_4$ (7ml), CH_3OH (400ml), HCl (15ml) in H_2O (30ml), was sprayed on pre-heated 76x25x1 mm chemically cleaned commercial glass substrate [5]. Initially, the tin oxide thin films were formed by changing nozzle-to-substrate distance from 20 to 40 cm in steps of 5 cm at 400°C (±2) substrate temperature. Subsequently, the nozzle-to-substrate distance was maintained at 30 cm, and thin films were deposited at different substrate temperatures, changed 380-440 °C in steps of 20 °C. Nozzle diameter and sprayed proportion at each cases were 0.2 mm and 8-10 ml/s, respectively. The film formation is an oxidation process as shown

$$SnCl_4 + O_2 \rightarrow SnO_2 + 2Cl_2$$

The solution was not atomized consecutively because the substrate temperature was lowered by spraying air, but atomized solution was occurred at short notice. After the substrate temperature returned to the desired level temperature, the spray process was repeated [12].

The crystallitinty and structure of SnO_2 thin films were obtained from their X-ray diffraction patterns. Diffraction data were collected by a Rigaku Rint 2000 diffractometer, with a constant sweep velocity of 6°/min, CuKα_1 radiation settings of 1.5405 Å, 40 kV, 30 mA. From the diffraction patterns, angle positions and relative intensities of Bragg reflections were determined. The preferred orientations of SnO_2 thin films were determined by the texture coefficient (TC). The surface morphology was carried out by a LEO 440 computer-controlled digital scanning electron microscope. The optical properties of SnO_2 thin films were investigated by a Perkim Elmer UV/VIS Lamda 2S spectrophotometer (λ =190-1100 nm) operating at room temperature. Optical constants such as refractive index n and extinction coefficient k were determined from the transmittance spectrum in the ultraviolet, visible and near-infrared (UV-VIS-NIR) regions using the envelope method [13,14]. The films were found to exhibit high transmittance (>90 %), low absorbance and low reflectance in the visible regions. Absorption coefficient α and the thickness of the film t were calculated from interference of transmittance spectra. The current-voltage (I-V) measurements were performed using HP4140B pA meter/DC voltage source, HP34401 Model Digital multimeter and Vee One Lab 6.1 computer program. Metal contacts were obtained by vacuum evaporation using a Leybold Heraus 300 Univex.

3. Results and discussion

3.1 Structural properties

The XRD patterns 2θ =20°-70° of all the films prepared at different nozzle-to-substrate distances and constant substrate temperature (400 °C) are shown in Fig.1. We observed (110), (101), (200), (211) and (301) peaks in all films, but peak intensities are different in each XRD data. The films are polycrystalline with (200) as dominant orientation. Another major orientations present are (110) and (211), while other orientations like (101) and (301) are also seen with comparatively lower intensities in the X-ray patterns. The best crystallization was observed with the nozzle-to-substrate distance 35 cm, at substrate temperature 400 ^oC.

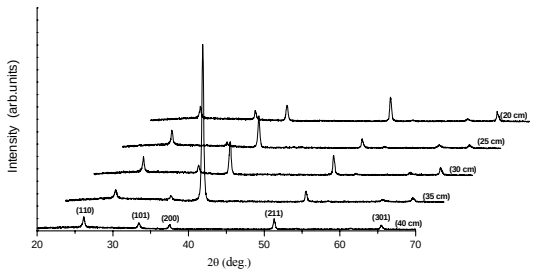

Fig. 1. The XRD patterns of SnO_2 thin films deposited on glass substrate (400 ^oC) at various substrates-to-nozzle distance.

The unit cell parameters and crystal structure were found via analytical methods using data obtained from X-ray diffraction pattern of SnO_2 thin films [15]. The crystal system was found as tetragonal rutile structure and also unit cell parameter values were calculated. The unit cell parameters calculated for each thin film are shown in Table 1. The calculated lattice parameters are in agreement with the values from literature (PDF card no:41-1445).

Table 1. The lattice parameters of tin oxide thin films.

Sprayed distance (cm)	Calculated		PDF (41-1445)	
	a=b (Å)	c (Å)	a =b (Å)	c (Å)
20	4.736	3.197	4.738	3.187
25	4.729	3.195	4.738	3.187
30	4.723	3.183	4.738	3.187
35	4.720	3.184	4.738	3.187
40	4.780	3.162	4.738	3.187

The texture coefficient defined by Barret and Massalski was used to determine the preferred orientation of the thin films. For a preferential orientation, the texture coefficient ($TC_{(hkl)}$) should be greater than one [16]. The $TC_{(hkl)}$ is given by;

$$TC_{(hkl)} = \frac{I_{(hkl)} / I_{o(hkl)}}{(1/n)\left[\sum_{i=1}^{n} \frac{I_{(hkl)}}{I_{o(hkl)}}\right]} \quad (1)$$

where TC is the texture coefficient for the (hkl) plane, I_{hkl} the measured intensity, I_o the corresponding standard intensity in the PDF cards for the powder [17], and n the number of diffraction peaks. Fig.2 shows variation of texture coefficient with nozzle-to-substrate distance.

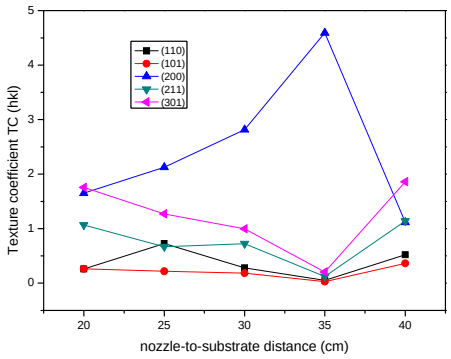

Fig. 2. Effect of nozzle-to-substrate distance on texture coefficient.

When Fig. 2 was examined, it was seen that TC(200) and TC(301) values increased and decreased at 20-35 cm distance, respectively, and in direct contradiction at 40 cm. TC values of (211), (110) and (101) peaks are indicated little variation with nozzle-to-substrate distance. (110) and (101) peaks were not of preferred orientation for TC values of mentioned peaks were lower than unity for all

the films. Because of the reason in above, the preferred orientation along the (200) peak presented at all distance. The texture coefficients for each (*hkl*) value are shown in Table 2.

Table 2. Effects of nozzle-to-distance on structure of tin oxide thin films.

(*hkl*)	Texture Coefficient					FWHM					Grain Size (*Å*)				
	Sprayed distance (cm)					Sprayed distance (cm)					Sprayed distance (cm)				
	20	25	30	35	40	20	25	30	35	40	20	25	30	35	40
(110)	0.261	0.291	0.280	0.051	0.521	0.275	0.263	0.255	0.299	0.313	318	335	348	290	275
(101)	0.263	0.127	0.184	0.029	0.363	0.243	0.166	0.267	0.326	0.266	375	625	336	268	337
(200)	1.650	3.062	2.815	4.592	1.115	0.282	0.263	0.277	0.259	0.249	319	345	325	352	368
(211)	1.068	0.355	0.725	0.122	1.140	0.234	0.225	0.224	0.256	0.220	417	438	439	374	451
(301)	1.756	0.517	0.995	0.206	1.861	0.229	0.327	0.265	0.311	0.271	460	304	386	322	376

The grain size of crystallites oriented along (hkl) planes can be calculated using Scherrer formula,

$$g = \frac{0.94\lambda}{B\cos\theta_B} \tag{2}$$

where λ is X-ray wavelength (0.15418 nm), B is FWHM of related (*hkl*) diffraction peak (in radians) and θ_B is Bragg diffraction angle [18]. The calculated crystallite size values for all samples are given in Table 2. It was seen that grain size didn't change linearly with nozzle-to-substrate distance. Generally, the grain size has a minimum value at 35 cm, and also the best crystalline was shown to be at 35 cm. Fig.3 a-e show SEM pictures of the thin films at various substrate-to-nozzle distances. All the SEM pictures are very similar expect figure e. The grain size varries most at 40 cm distance.

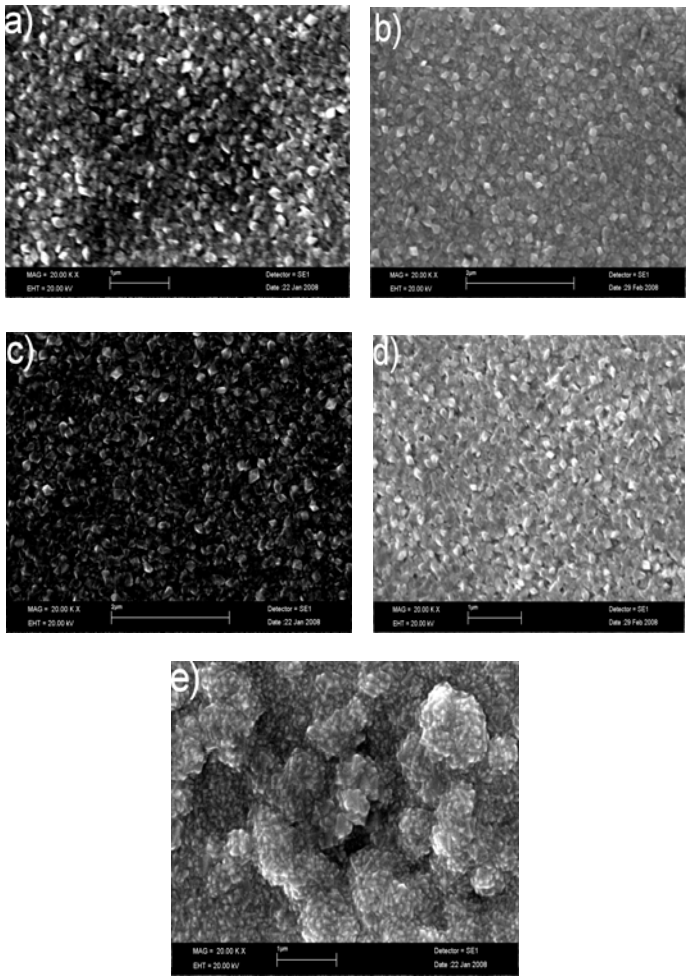

Fig.3. SEM pictures of tin oxide thin films deposited at various nozzle distances a) 20 cm, b) 25 cm, c) 30 cm, d) 35 cm and e) 40 cm.

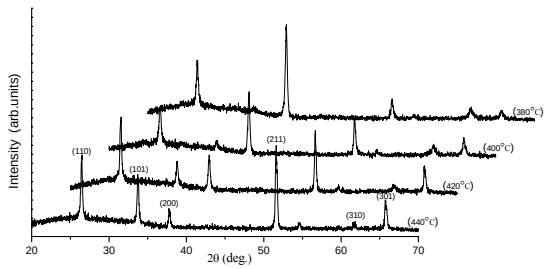

Fig. 4. The XRD patterns of SnO_2 thin films deposited on glass substrate at various temperatures.

The XRD patterns of SnO_2 thin films prepared at different temperatures are shown in Fig. 4. All of the XRD patterns show crystallization at tetragonal rutile structure. The lower the temperature the greater the increase of the (200) peak. However, the other peaks decreased with decreasing temperatures. The calculated lattice parameters of tin oxide thin films are shown in Table 3. It is shown that values calculated and PDF values are approximately equivalent.

Table 3. The lattice parameters of tin oxide thin films.

Substrate Temperature (°C)	Calculated		PDF (41-1445)	
	a=b(Å)	*c(Å)*	*a=b(Å)*	*c(Å)*
380	4.744	3.180	4.738	3.187
400	4.723	3.183	4.738	3.187
420	4.739	3.201	4.738	3.187
440	4.763	3.202	4.738	3.187

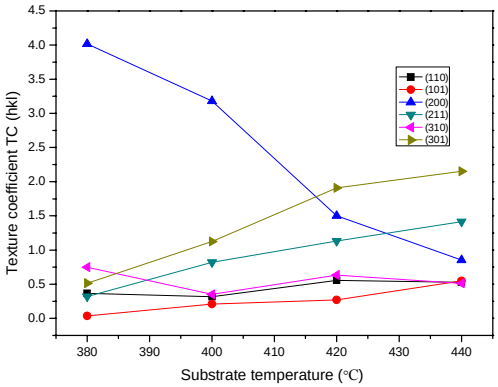

Fig. 5. Effect of substrate temperature on texture coefficient.

Fig. 5 shows that the texture coefficient of (200) peak decrease with increasing temperature, but texture coefficients of the other peaks increase with increasing temperature. For example, the texture coefficients of (211) and (301) peaks increased from 0.319 to 1.414 and from 0.513 to 2.151, respectively. The effect of temperature on structure of tin oxide thin films is shown in Table 4.

Table 4. Effects of temperature on structure of tin oxide thin films.

(*hkl*)	Texture Coefficient				FWHM				Grain size (*Å*)			
	Substrate temperature (°C)				Substrate temperature (°C)				Substrate temperature (°C)			
	380	400	420	440	380	400	420	440	380	400	420	440
(110)	0.366	0.317	0.556	0.526	0.282	0.255	0.245	0.239	309	348	366	377
(101)	0.035	0.208	0.271	0.547	0.149	0.267	0.235	0.212	748	336	390	445
(200)	4.018	3.181	1.50	0.851	0.265	0.277	0.276	0.209	342	325	326	458
(211)	0.319	0.819	1.131	1.414	0.322	0.224	0.228	0.207	288	439	430	488
(310)	0.748	0.350	0.632	0.511	0.427	0.357	0.343	0.347	223	270	282	278
(301)	0.513	1.124	1.909	2.151	0.433	0.265	0.208	0.222	225	386	520	478

SEM pictures of thin films deposited at 380 °C, 400 °C, 420 °C and 440 °C are shown Fig.6. As seen in Fig.6, porosity percentage of tin oxide thin films increased with raising temperature.

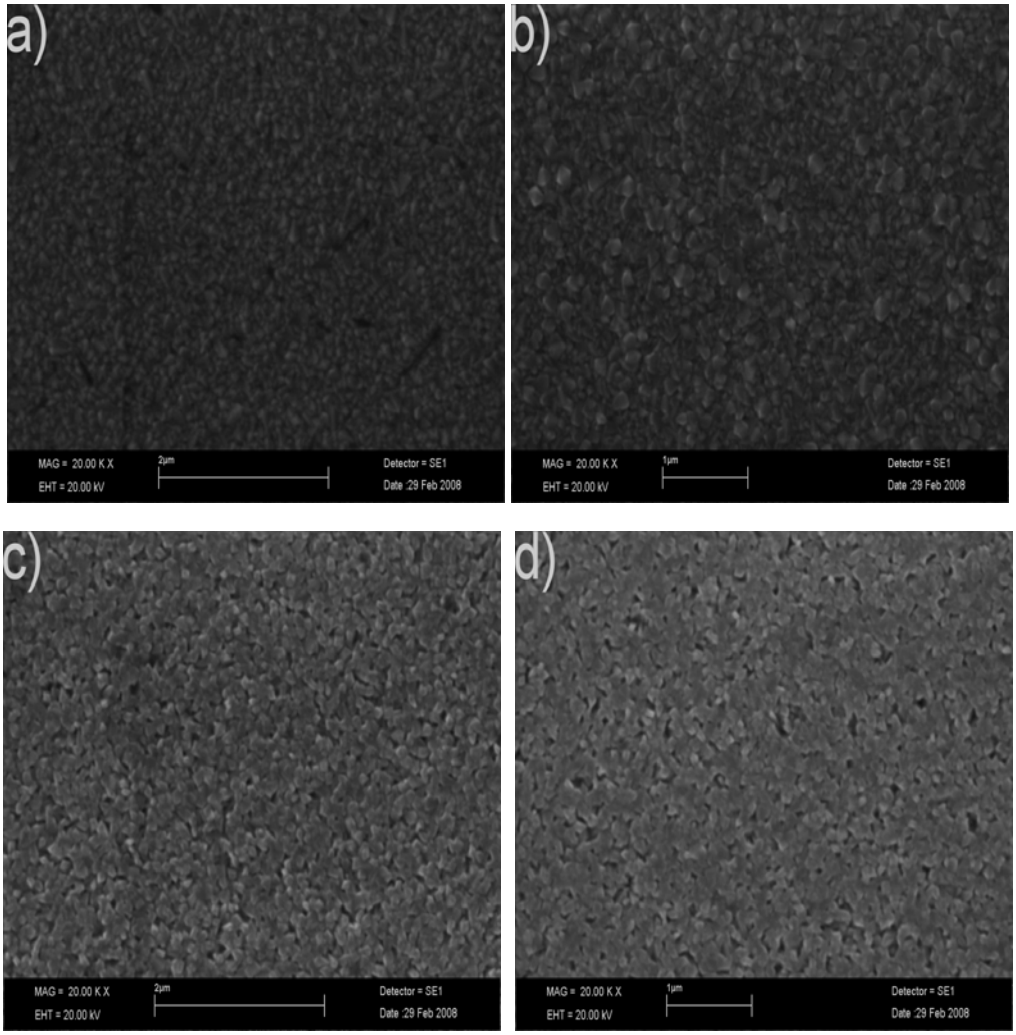

Fig. 6. SEM pictures of tin oxide thin films obtained at various substrate temperatures, a) 380 °C, b) 400 °C, c) 420 °C and d) 440 °C.

3. 2 Optical properties

The optical transmittance of SnO_2 thin films obtained at different sprayed distances which range between 20-40 cm at 400 °C are shown in Fig. 7. The spectra are recorded for the wavelength range between 200 to 1100 nm at room temperature. The optical transmittance values of the thin films varies for the wavelengths range 400-1100 nm with an average transmittance value of % 90. The transmission spectra of all samples have higher transmittance values and more interference fringes than those in the previous studies [19].

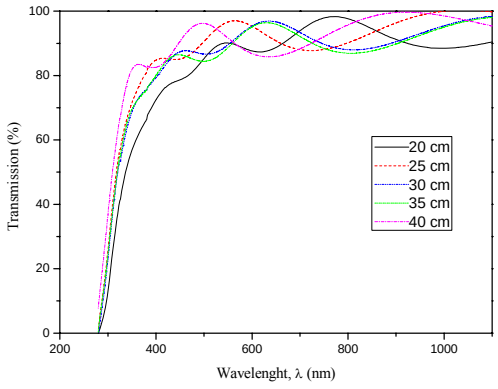

Fig. 7. The optical transmission curves of SnO_2 thin films at different nozzle-to-substrate distances.

While transmission curves of the films at the substrate-to-nozzle distances of 30 and 35 cm were similar, X-ray diffraction data showed worse crystallization of the thin films grown at 30 cm than those grown at 35 cm. The value of the film thickness was determined by utilizing the optical transmission curves of in Fig. 7 by using the following relation;

$$t = \frac{\lambda_1 \lambda_2}{2\left[n(\lambda_1)\lambda_2 - n(\lambda_2)\lambda_1\right]} \tag{3}$$

where $n(\lambda_1)$ and $n(\lambda_2)$ are the refractive indices at the two adjacent maxima (or minima) at λ_1 and λ_2. The thickness of the SnO_2 thin films were found to be 0.41-1.11 μm.

The optical constants were found from an optical transmittance curve of SnO_2 thin films using the envelope method [20]. First of all, the refractive index was calculated from the following equations;

$$n = \left[N + (N^2 - n_s^2)^{1/2}\right]^{1/2}$$
$$N = \frac{(n^2+1)}{2} + 2n_s \frac{(T_{\max} - T_{\min})}{T_{\max} T_{\min}} \tag{4}$$

where n_s is refractive index of the substrate, $T_{\max}$ and $T_{\min}$ are maximum and minimum transmittances at the same wavelength in fitted envelope curves on the transmittance curves.

The values of refractive index were calculated for wavelengths between 400-1100 nm for SnO_2 thin films and the variations are shown in Fig. 8. The refractive index increases from 1.76 to 1.92 in the range of 400 to1100 nm. The refractive index was measured to be 1.90 for the wavelengths from 550 to 700 nm which is consistent with the standard value in the literature [21]. Refractive index and extinction coefficient values of the thin films grown at 380-440 °C were found to be 1.57-1.93, 0.096-0.36, respectively.

The extinction coefficient can be calculated by the following equations;

$$k = \frac{\alpha\lambda}{4\pi} \tag{5}$$

$$\alpha = \frac{1}{t}\ln\frac{(n-1)(n-n_s)\left[(T_{\max}/T_{\min})^{1/2}+1\right]}{(n+1)(n-n_s)\left[(T_{\max}/T_{\min})^{1/2}-1\right]} \tag{6}$$

where α is the absorption coefficient and t is the film thickness. The variation of extinction coefficient with wavelength is shown in Fig.8. For wavelengths ranging between 400-1100 nm the extinction coefficient increased linearly from 0.14 to 0.31.

To find the energy band gap of SnO_2 thin films, the equation below was taken into consideration;

$$\alpha h\gamma = K(h\gamma - E_g)^{1/2} \tag{7}$$

where α is the absorption coefficient, K is a constant, $h\nu$ is the energy of the incident photon, E_g is energy gap. The absorption coefficient of the films was calculated using the following expression;

$$\alpha = -\frac{1}{t}\ln\left(\frac{T}{T_o}\right) \tag{8}$$

where t is film thickness, T is normalized transmittance. Because the envelope method is not valid in the strong absorption region, the absorption coefficient α of SnO_2 thin films was defined from the transmittance measurements instead of Eq. 6. After the absorption coefficient was found, for samples prepared at 40 cm distance a graph of α^2 versus $h\nu$ was ploted as shown in Fig. 9. The band gap (E_g) is determined by extrapolating the straight-line portion to the energy axis. The intercept on x axis value gives the energy gap, for all samples this value lies in the range from 3.99 to 4.11 eV. This is in good agreement with previous result [22].

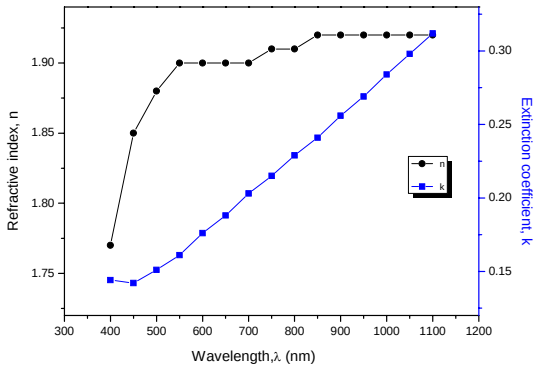

Fig. 8. Variation of refractive index n and extinction coefficient k versus wavelength at 40 cm nozzle-to-substrate distance and 400 °C substrate temperature.

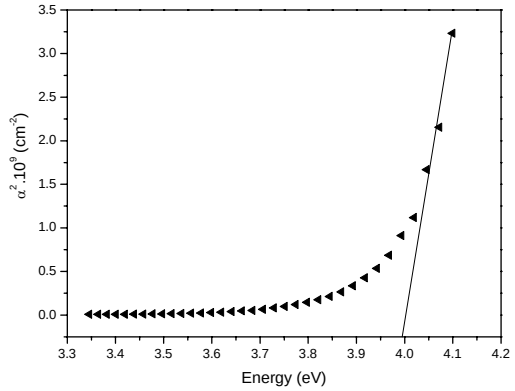

Fig. 9. Variation of α^2 versus photon energy $h\nu$ for SnO_2 thin film (at 40 cm nozzle-to-substrate distance).

3. 3 Electrical properties

I-V characteristics of the SnO_2 film are shown in Fig 10. Surface type (planar) Au contacts were made for electrical measurements. The current values of the films were measured at room temperature and in the dark by applying voltage values between 0.1 and 100 V. The ohmic current mechanism is dominant for SnO_2 films.

The electrical conductivities of the films were calculated using Ohm's law given by;

$$R = \rho \frac{L}{A} \tag{9}$$

where R is the electrical resistance, ρ is the electrical resistivity and L is the length sample, A is the cross-section area. The calculated electrical resistivity value is ρ=(2.47-7.13)·10^{-4} Ωcm for the deposited film. This value is consistent with ref. [23].

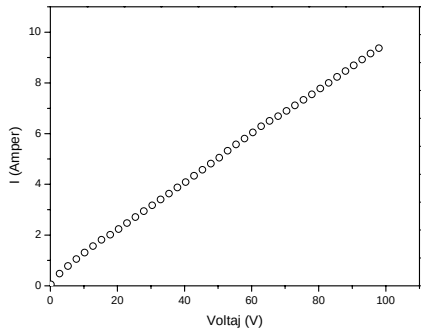

Fig. 10. The I-V characteristics of the SnO_2 film.

4. Conclusions

Highly trasparent SnO_2 thin films were deposited on glass substrate by spray pyrolysis method investigated at different substrate-to-nozzle distances. The best crystallization was observed at 35 cm, while the substrate temperature was kept at 400 °C. The crystallographic structures and unit cell parameters of the thin films were found as tetragonal rutile, and it was found that substrate-to-nozzle distance did not affect crystallographic structure. It was found that texture coefficient of the (200) peak was greater than the one at each of the distances. The average grain size of the films were calculated by using the Sherrer formula. The SEM analysis of tin oxide thin films indicated that the surface topologies of thin films were roughly similar to each other except for those deposited at 40 cm substrate-to-nozzle distance. According to SEM results, topological properties also changed with temperature. The wavelength dependence of the index of refraction, the extinction coefficient and the thickness of the SnO_2 thin films were calculated from the transmission curve using the envelope method. From the X-ray diffraction pattern, peak densities and values of texture coefficient increased gradually with increasing temperature except for the (200) peak. The electrical resistivity of the films were calculated by using Ohm's law.

Acknowledgments

This work was supported by Cukurova University under FEF2006BAP10 project number. The authors to thanks Ihsan Aksit and Altınay Boyraz for SEM studies.

References

[1] B. Ahn, S. Oh, C. Lee, G. Kim, H. Kim, S. Lee, J. Cryst. Grow. **309**, 128 (2007).
[2] H. L. Ma, X. T. Hao, J. Ma, Y. G. Yang, J. Huang, D. H. Zhang, X. G. Xu, Appl. Surf. Sci. **191**, 313 (2002).
[3] T. K. Subramanyam, S. Ulthanna, B. S. Naidu, Mater. Lett. **35**, 214 (1998).
[4] C. Agashe, B. R. Marathe, M. G. Takwale, V. G. Bhide, Thin Solid Films **164**, 261 (1988).
[5] E. Çetinörgü, C. Gumus, S. Goldsmith, F. Mansur, Appl. and Mater. Sci. **10**, 3278 (2007).
[6] H. Han, Q. Zhou, J. Wang, Mater. Lett. **60**, 252 (2006).
[7] T. M. Racheva, G. W. Critchlow, Thin Solid Films **292**, 299 (1997).
[8] A. K. Mukhopadhyay, P. Mitra, A. P. Chatterjee, H. S. Maiti, Ceram. Int. **26**, 123 (2000).
[9] A. Pereira, L. Cultrera, A. Dima, M. Susu, A. Perrone, H. L. Du, A. O. Volkov, R. Cutting, P. K. Datta, Thin Solid Films **497**, 142 (2006).
[10] P. S. Patil, S. B. Sadale, S. H. Mujawar, P. S. Shinde, P. S. Chigare, Appl. Surf. Sci. **253**, 8560 (2007).
[11] C. Gümüs, O. M. Ozkendir, H. Kavak, Y. Ufuktepe, J. Optoelectron. Adv. Mater. **8**, 299 (2006).
[12] K. Murakami, K. Nakajima, S. Kaneko, Thin Solid Films **515**, 8632 (2007).
[13] J. C. Manifacier, J. Gasiot, J. P. Fillard, J. Phys. E: Sci. Instrum. **9**, 1002 (1976).
[14] R. Swanepoel, J. Phys. E: Sci. Instrum. **16**, 1214 (1983).
[15] V. Azaroff, M. Buerger, The Powder Method in X-Ray Crystallography, Mc.Graww-Hill Book Company, New York (1958).
[16] J. P. Nair, R. Jayakrishnan, N. B. Chaure, R. K. Pandey, Semicond. Sci.Technol. **13**, 340 (1998).
[17] Joint Committee on Powder Diffraction Standarts, Powder Diffraction File, cards no:41-1445.
[18] C. Gumus, C. Ulutas, Y. Ufuktepe, Opt. Mater. **29**, 1183 (2007).
[19] S. Lee, B. Park, Thin Solid Films **510**, 154 (2006).
[20] J. Müllerova, J. Mudron, Acta Physical Slovaca **50**, 477 (2000).
[21] H. Demiryont., K. Nietering, R. Surowiec, F. I. Brown, D. R. Platts, Appl. Opt. **18**, 3803 (1987).
[22] A. K. Abass, M. T. Mohammad, J. Appl. Phys. 59 (5), **1641** (1986).
[23] K. H. Yoon, J. S. Song, Sol. Energy Mater. and Sol. Cells **28**, 317 (1993)

* Corresponding author: cgumus@cu.edu.tr